Experimental Mechanics
DOI 10.1007/s11340-011-9544-6

Directional Wave Propagation in a Highly Nonlinear Square Packing of Spheres

A. Leonard · F. Fraternali · C. Daraio

Received: 16 July 2011 / Accepted: 29 August 2011

Abstract We studied the dynamic response of a two-dimensional square packing of uncompressed stainless steel spheres excited by impulsive loadings. We developed a new experimental measurement technique, employing miniature tri-axial accelerometers, to determine the stress wave properties in the array resulting from both an in-plane and out-of-plane impact. Results from our numerical simulations, based on a discrete particle model, were in good agreement with the experimental results. We observed that the impulsive excitations were resolved into solitary waves traveling only through initially excited chains. The observed solitary waves were determined to have similar (Hertzian) properties to the extensively studied solitary waves supported by an uncompressed, uniform, one-dimensional chain of spheres. The highly directional response of this system could be used as a basis to design granular crystals with predetermined wave propagation paths capable of mitigating stress wave energy.

Keywords Two-dimensional square packing · Granular crystals · Highly nonlinear dynamics · Directional wave propagation · Impulsive excitation

A. Leonard · C. Daraio (✉)
Department of Engineering and Applied Science,
California Institute of Technology,
Pasadena, CA 91125, USA
e-mail: daraio@caltech.edu

A. Leonard
e-mail: andreal@caltech.edu

F. Fraternali
Department of Civil Engineering,
University of Salerno, 84084 Fisciano, SA, Italy
e-mail: f.fraternali@unisa.it

Introduction

The dynamic behavior of uncompressed, one-dimensional uniform chains of spheres in contact (i.e. granular crystals) has been extensively studied [1–7]. In the elastic limit, these systems have been shown to support the formation and propagation of solitary waves [1–3]. Heterogeneous one-dimensional chains of spheres have also been studied and proposed as materials for impulse or vibration mitigation [2, 8–14]. It was found that the presence of defects and interfaces causes energy scattering [11, 15, 16], trapping [17] and anomalous reflections [12]. The extension of these studies in higher-dimensional systems could enable the discovery of richer physical phenomena and the design of materials for different engineering applications. The study of two-dimensional, highly nonlinear granular crystals has not been extensively explored. This work studies the stress wave properties in a basic two-dimensional granular crystal. We study a simple square packing as a quasi-one-dimensional system, and compare its response with the available theoretical and numerical frameworks [2]. We present a new experimental setup to study multidirectional wave propagation, based on the use of tri-axial accelerometers. This approach will be extended to the study of more complex two-dimensional systems and to different packing geometries.

1-D Theoretical Background

The wave motion supported by one-dimensional granular crystals was first described by Nesterenko using a long wavelength approximation. The fundamental

Published online: 06 October 2011

wave equation derived for the highly nonlinear response of uncompressed particles is,

$$u_{tt} = -c^2 \left\{ (-u_x)^{\frac{3}{2}} + \frac{2R^2}{5} \left[(-u_x)^{\frac{1}{4}} \left((-u_x)^{\frac{5}{4}} \right)_{xx} \right] \right\}_x, \quad (1)$$

where u represents the displacement of the center of each sphere from its equilibrium position and $c^2 = \frac{2E}{\pi\rho(1-\nu^2)}$ [2]. Here R, E, ρ, and ν, are the radius, Young's Modulus, density, and Poisson's ratio of the particles.

The propagating wave in the highly nonlinear regime can be described by a single hump of the periodic solution of equation (1) [1, 2]:

$$v = V_s \left(\frac{5V_s^2}{4c^2} \right)^2 \cos^4 \left(\frac{\sqrt{10}}{10R} x \right), \quad (2)$$

where v is the particle velocity and V_s is the wave speed. This solitary wave has a fixed wavelength of approximately 5 particle diameters and a wave speed that depends on its amplitude [1, 2, 6]:

$$V_s = \left(\frac{16}{25} \right)^{\frac{1}{5}} c^{\frac{4}{5}} v_m^{\frac{1}{5}} = 0.68 \left(\frac{E}{R\rho^{\frac{3}{2}} \left(1-\nu^2\right)} \right)^{\frac{1}{3}} F_m^{\frac{1}{6}}, \quad (3)$$

where v_m is the maximum particle velocity and F_m the maximum compressive contact force. The existence of this compact solitary wave was first shown experimentally by Lazaridi and Nesterenko [3] and later confirmed experimentally [4–6, 10] and numerically [7, 13, 16, 18–21] by others. Additional studies related to the wave amplitude-wave speed scaling relation for uniform, uncompressed one-dimensional chains of spheres have confirmed both numerically [20, 21] and experimentally [4, 5, 20] Nesterenko's analytic results (first half of equation (3)).

2-D Background

For a simple cubic packing of spheres, Nesterenko suggested that waves should propagate similar to the one-dimensional case when the packing is excited parallel to the array of chains [2]. However, this has not been quantitatively verified experimentally until now. Past studies of the dynamic behavior of highly ordered two-dimensional granular crystals primarily focused on hexagonal packings [22–29], with very few studies considering square packings [25, 26]. Additionally, studies concerning the amplitude-wave speed scaling relationship of highly ordered granular crystals consisted of hexagonal packings of spheres [22–24, 30].

Numerical simulations employing the discrete element method (DEM) were used to study the stress wave propagation of uncompressed, two-dimensional granular crystals and were shown to be in good agreement with experimental results [25–28, 31]. Sadd et al. used DEM simulations to investigate the stress wave propagation in a granular array of elliptical disks [26]. Past experiments on various packings of photoelastic elliptical disks concluded that contact normals and the vectors connecting particles' centers of mass influence wave propagation characteristics, such as load transfer path and load attenuation [25]. Specifically, Zhu et al. studied a square packing of elliptical disks and observed that the wave propagation was highly directional. They observed that inaccuracy of particle spacial arrangement attributed to only small amounts of energy transfer, if any, into chains adjacent to those initially excited in experiments (similar to what we observe in this work). More recently, Nishida et al. used DEM simulations to model the dynamic response of a two-dimensional hexagonal packing excited by a high velocity spherical projectile [28], and were able to obtain good agreement with experiments when comparing force history profiles along the opposite edge of the specimen.

Quantitative studies of wave propagation in two-dimensional granular crystals present experimental challenges. For example, because of geometrical tolerances on the particles' shape, it is difficult to assemble an ordered packing reproducing the ideal configuration. In the ideal configuration, all particles have an equal number of contacts and equal equilibrium forces. However, in experiments if, for example, a single particle is too small, there will be a loss of contacts between neighboring particles. Additionally, if a single particle is too large, local compressive forces may exist at surrounding particle contacts. Several past works studied the effects of imperfections in two-dimensional granular crystals and their role in the stress wave propagation [22–24, 30]. While Herztian behavior predicts a $n = \frac{1}{6}$ power-law between maximum force and wave speed (equation (3)), it was found that the presence of defects tends to increase the wave propagation speed ($n = \frac{1}{4}$ instead of $\frac{1}{6}$), effectively inducing deviations from the theoretical Hertzian behavior. This deviation from Hertzian behavior was observed only for granular crystals with low precompression. Increasing the precompression applied on hexagonal arrays was seen to cause a transition to a fully Hertzian behavior [22–24, 30]. Future work on the dynamic behavior of highly ordered uncompressed two-dimensional granular crystals will be needed to fully understand the quantitative stress wave front properties in these systems, and to characterize how these properties depend on the underlying particle arrangement.

Recently, Daraio et al. looked at the pulse splitting and recombination in a y-shaped granular network [32]. They demonstrated the ability to bend and split incident pulses, further suggesting the ability of granular systems to redirect mechanical energy.

Experimental Setup

Experiments were performed on granular crystals assembled within a confining box composed of a flat polycarbonate bottom and delrin-lined walls. The array of particles consisted of a 20 by 20 square packing of stainless steel spheres. In order to achieve a uniform contact lattice, a slight tilt (less than 5 degrees) was applied to both the x- and y-directions. Two different impact conditions were considered: (1) in-plane, where the array was impacted between the two middle particles along the edge, and (2) out-of-plane, where the array was impacted between the four spheres at the center of the array (see Fig. 1). The system was excited impulsively by a stainless steel striker sphere, identical to the particles composing the crystal, impacting a resting striker sphere in direct contact with the array. The presence of the resting striker sphere allowed us to achieve a more repeatable, uniform impact compared to the striker sphere directly impacting the array. For the in-plane impacts, a solenoid was used to impact the striker sphere, giving it a repeatable initial velocity. The striker's velocity was then measured with an optical velocimeter just before impacting the system. For the out-of-plane impacts, the striker sphere was dropped from some known height (through guide rails), and its initial velocity was calculated from the drop height.

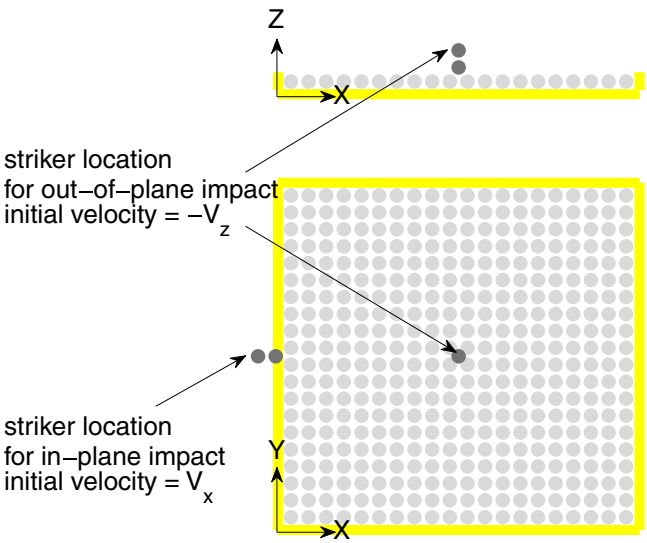

Fig. 1 Schematic diagrams of the test configurations: (*Top*) view of the setup from the side, showing the position of the striker spheres (*dark grey*) and (*Bottom*) view of the setup from the top. The square array was a 20 by 20 packing of 19.05 mm diameter spheres. For the in-plane impacts, the striker sphere impacted the resting striker sphere in contact with edge particles X_1Y_{10} and X_1Y_{11}. For out-of-plane impacts, the striker sphere impacted the resting striker sphere in contact with central particles $X_{10}Y_{10}$, $X_{11}Y_{10}$, $X_{10}Y_{11}$, and $X_{11}Y_{11}$

Custom fabricated sensor particles (Fig. 2) replaced solid spheres at selected locations in the system to measure the particles' motion. These sensor particles consisted of a sphere with a central hole drilled in order to embed a pre-calibrated miniature tri-axial accelerometer (PCB 356A01 with sensitivity 0.51 mV/(m/s^2)). The accelerometers required a signal conditioner (PCB 481A02) before being connected with the data acquisition board (NI BNC-2110 and NI PCI-6123 with simultaneous sampling rate up to 500 kS/s). The acceleration output from the sensor particles was directly compared with the acceleration of the center of mass of each particle obtained from the numerical simulations.

Previous experiments measured either the response along the edge of the granular crystal [3–5, 22, 28], the one-dimensional force components within the spheres [6, 15, 16, 20], or required significant post-processing in order to obtain two-dimensional measurements from photoelastic particles [25, 33–36]. The use of tri-axial accelerometers allows for quick and accurate measurements of the response of individual particles in the granular crystals.

The use of accelerometers embedded inside selected particles did not alter the Hertzian contact between the sensor particles and their neighboring elements. However, the average mass of the solid stainless steel spheres was 28.79 g, whereas the average mass of the assembled sensor particles was 26.52 g (approximately 92% of the solid sphere mass). Recent experimental and simulation studies of mass defects in a

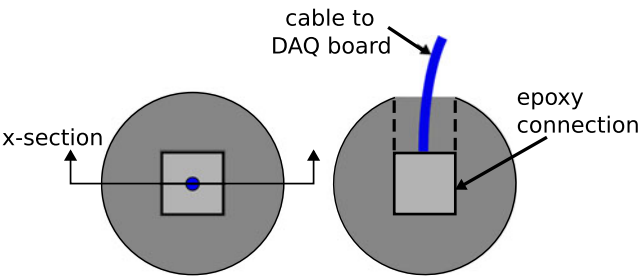

Fig. 2 Schematic diagram of the assembled sensor particle: (*Left*) top view and (*Right*) cross-section view. The accelerometer is a 6.35 mm cube and the sphere is 19.05 mm in diameter

one-dimensional, uncompressed chain of spheres have shown the presence of a localized mode as a result of traveling solitary waves interacting with a light mass intruder [15]. We performed systematic numerical simulations and experiments to determine the effect of the mass difference and the influence of the sensor particles on the propagation of the impulses in a one-dimensional model system.

Numerical simulations were performed on a horizontal chain of 20 stainless steel particles impacted by an identical striker particle and bounded by a soft (delrin) wall at the far end. The 10th particle's mass was then varied from 50% to 100% of the solid (19.05 mm diameter) stainless steel sphere mass, while keeping the radius constant. As the mass of the tenth particle was decreased, a series of reflected waves around the light mass defect begin to emerge and grow in amplitude. It was determined that for an 8% mass reduction, as the one present in our experimental system, the amplitude of the largest reflection was less than 1.2% of the incident solitary wave amplitude. Since this reflection amplitude is potentially near the noise level observed in experiments (depending on the magnitude of excitation) it is reasonable to consider this phenomenon as having a negligible effect on the studied two-dimensional systems.

To confirm this hypothesis, we performed an experimental study to determine the effect of the sensor particles replacing solid spheres. A nearly horizontal one-dimensional chain of 20 stainless steel spheres was assembled between two polycarbonate guide rails. A slight tilt (less than 5 degrees) was induced to ensure contact between all spheres. The chain was impacted by a striker particle, identical to those in the chain. The striker sphere was impacted by a solenoid to give it a repeatable initial velocity. At the far end of the chain, a dynamic load cell (PCB 208C02 with sensitivity 11,241 mV/kN) was placed in between a heavy mass aluminum block and the last particle. The baseline response (the case of no sensor particles) at the end of the chain was then compared with the force felt at the wall when sensor particles replaced the (a) 6th, (b) 11th, (c) 16th, (d) 11th and 16th, and (e) 6th, 11th, and 16th solid spheres. The experiment was repeated ten times for each configuration. No measurable variation in wavelength was seen and no clear trend was observed in the variation of wave amplitude at the wall when sensor particles were introduced in the system. In conclusion, there was no clear indication that the sensor particles measurably altered the response of the system, validating their use for additional studies.

In the two-dimensional setup, these sensors were used to measure the dynamic response of the granular crystal when subjected to both in-plane and out-of-plane impacts. The recorded experimental measurements were triggered when the excitation reached the first sensor particle. In numerical simulations the zero time represents the moment of striker impact. In order to compare experimental data with numerical simulations the experimental zero time was obtained using the measured wave speed and the known distance of the first sensor from the impact. Additional experiments were then performed for a variety of impact velocities in order to determined the amplitude-wave speed relationship and the wavelengths of the traveling pulses.

Numerical Simulations

Numerical simulations were performed using a three-dimensional discrete particle model, in which each sphere was modeled as a point mass connected by nonlinear (Herztian [37]) springs. The simulations in this work used a forth order Runge Kutta scheme to integrate the nonlinear system of differential equations [2]:

$$m_i\ddot{u}_i = A_{i,j_-}\left((R_i + R_{j_-}) - (x_i - x_{j_-})\right)_+^{\frac{3}{2}} - A_{i,j_+}\left((R_i + R_{j_+}) - (x_{j_+} - x_i)\right)_+^{\frac{3}{2}}, \quad (4)$$

where $A_{i,j} = \frac{4}{3}\left(\frac{1-\nu_i^2}{E_i} + \frac{1-\nu_j^2}{E_j}\right)^{-1}\left(\frac{R_i R_j}{R_i+R_j}\right)^{\frac{1}{2}}$ and x_i represents either the x, y, or z position of the center of sphere i, which is in contact with j neighboring spheres (where the j_- and j_+ neighbors have center locations in the negative and positive x_i directions, respectively). The notation $(\triangle x)_+$ is used to describe the lack of stiffness in tension, where $(\triangle x)_+ = \triangle x$ for $\triangle x \geq 0$ and $(\triangle x)_+ = 0$ otherwise. Walls were modeled as spherical particles of infinite radius. The effects of gravity [38] and dissipative losses present in experiments [39] were neglected in the numerical simulations. The material properties used in the calculations can be found in Table 1. We used experimentally measured impact velocities as input in the simulations.

Table 1 Material properties (www.mcmaster.com, www.matweb.com, www.ePlastics.com)

Material	Mass density (kg/m^3)	Young's modulus (GPa)	Poisson's ratio
Stainless steel (type 316)	8,000	193	0.3
Delrin	1,400	3.1	0.35
Polycarbonate	1,200	2.3	0.37

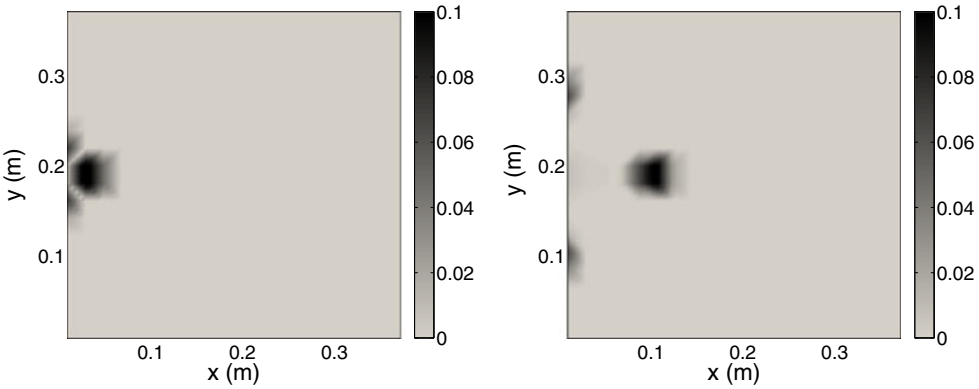

Fig. 3 Density plots corresponding to the amplitude of the particle velocity obtained from numerical simulations as a function of spacial position in the granular crystal. (*Left*) At 0.15 ms and (*Right*) at 0.30 ms after the array was impacted in-plane with a striker velocity $V_x = 0.29$ m/s. The *grey-scale* indicates the particle velocity amplitude in m/s

Results and Discussion

It is expected that under the impact conditions the square packing should behave similarly to a simple one-dimensional chain [1, 2]. For both in-plane and out-of-plane impacts, we observed that the impulsive excitations were resolved into solitary waves traveling through only initially excited chains of spheres. The properties of the traveling waves, including pulse length and the dependenace of wave speed on the maximum particle velocity, were calculated for experiments and numerical simulations. We found that the solitary waves propagating in these two-dimensional granular crystals had similar properties to those previously observed in accordance with Nesterenko's well know highly nonlinear one-dimensional theory [1, 2].

Wave Propagation Path

When the square array was impacted in-plane, we observed solitary waves traveling through four chains: one through each of the two central chains and one through each of the two edge chains (Fig. 3). Numerical simulations revealed that of the total energy input into the system (by the striker spheres initial velocity), 71.5% went into the solitary waves traveling in the two central chains along the impact direction, and 24.5% into the waves traveling transversely through the edge chains. The remaining energy was lost in the rebounding of the striker spheres and the particles nearest the impact. In experiments, sensor particles were placed at selected locations within the granular crystal to capture the waves traveling through each of these chains. The signal recorded by the sensors was compared with numerical simulations. Figure 4 describes the motion of the particles in the two central chains and Fig. 5 describes the motion of the particles in the two edge chains resulting from the in-plane impact. Experiments were repeated

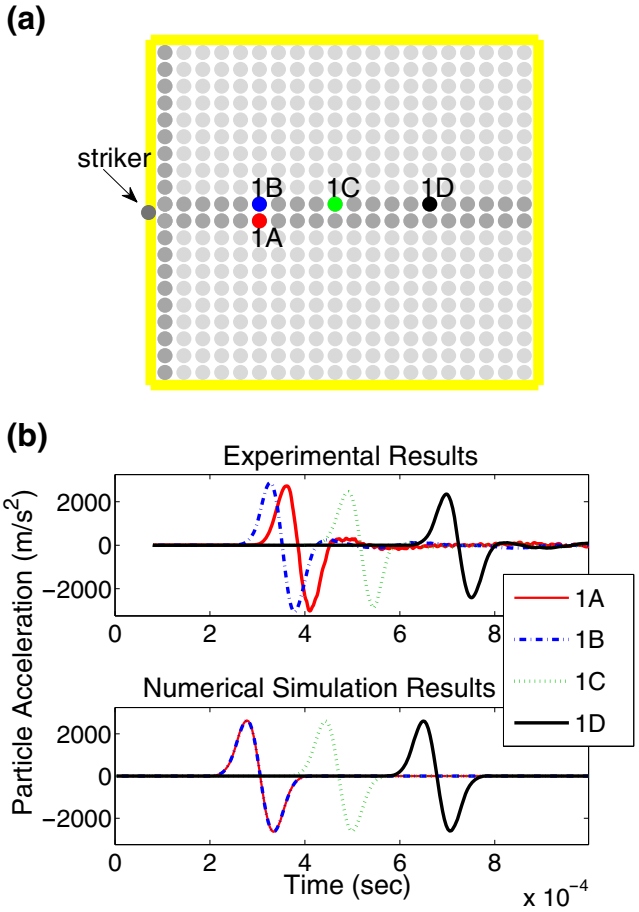

Fig. 4 Experimental and numerical simulation responses of the two central chains in the granular crystal resulting from an in-plane impact. (**a**) Schematic diagram showing the experimental setup and the positions of the sensor particles (*shaded spheres* indicate particles excited by the impulse). (**b**) Signals recorded at the sensor locations. The *top panel* represents experimental results and the *bottom panel* the numerical simulations. In both experiments and simulations each particle's acceleration in the x-direction is plotted as a function of time. The experimental y-acceleration was nearly zero for all sensor locations (zero in simulations) and was therefore not plotted

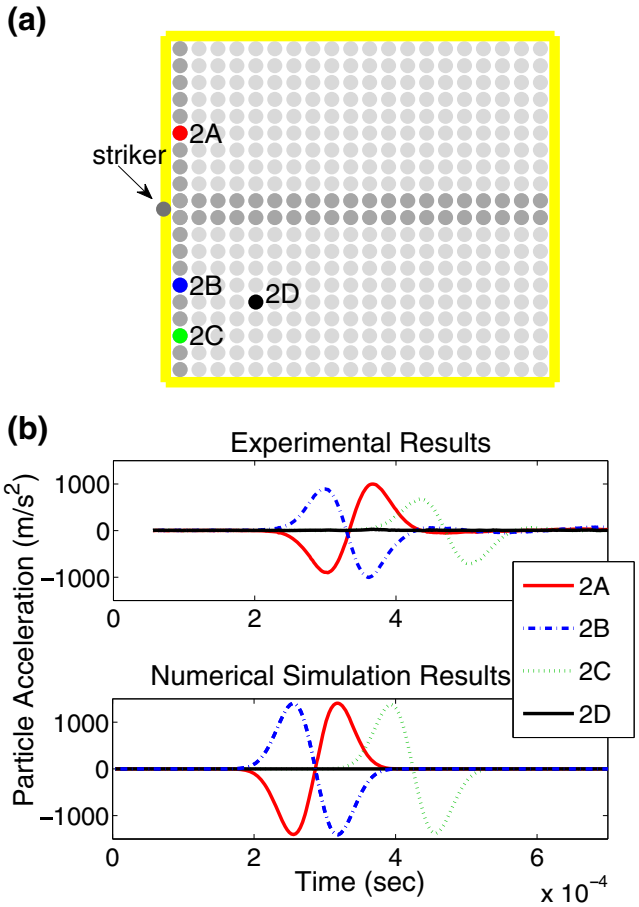

Fig. 5 Experimental and numerical simulation responses of the two edge chains in the granular crystal resulting from an in-plane impact. (**a**) Schematic diagram showing the experimental setup and the positions of the sensor particles (*shaded spheres* indicate particles excited by the impulse). (**b**) Signals recorded at the sensor locations. The *top panel* represents experimental results and the *bottom panel* the numerical simulations. In both experiments and simulations the particle's acceleration obtained from sensors 2A, 2B, and 2C in the negative y-direction is plotted as a function of time. The experimental x-acceleration was nearly zero for all sensor locations (zero in simulations) and was therefore not plotted. The signal plotted for sensor 2D includes the total magnitude of the x- and y-particle acceleration

15 times for each sensor configuration, with an average striker velocity of $V_x = 0.29$ m/s.

To capture the waves traveling through the central chains after the in-plane impact, sensors 1A and 1B were located six particles from the impact in each of the two central chains. Additional sensors were placed in one of the central chains at ten and fifteen particles from the impact (sensors 1C and 1D in Fig. 4(a)). Figure 4(b) compares the experimental acceleration recorded at these sensor locations with those obtained from numerical simulations. Due to the systems symmetry, we expected an identical response for sensors 1A and 1B in the central chains. However, slight variations in signal arrival times and amplitudes were observed in experiments. These variations were most likely an effect of imperfect striker impacts. If the striker does not impact each of the two edge spheres simultaneously (because of slight misalignment) the result should be a slight time delay and uneven force transmission between adjacent chains, similar to what was observed in experiments. In the central chain, the difference in time of arrival of peak particle acceleration ($t_{\text{peak}}(1B) - t_{\text{peak}}(1A)$) was $-21(\pm 68)$ microseconds and the percent difference in peak acceleration of sensor $1A$ with respect to sensor $1B$ was $4\%(\pm 10\%)$. The experimental results shown in Fig. 4(b) best represent the average response of the system from the 15 repeated experiments (this signal most closely represent the mean values for both peak arrival time and percent amplitude of the mentioned sensor pairs).

To capture the waves traveling transversely through the two edge chains after the in-plane impact, sensors 2A and 2B were placed five particles from the impact in each of the two edge chains and another sensor was placed in one of the edge chains at eight particles from the impact (2C in Fig. 5(a)). Additionally, we placed a sensor particle several diameters away from the waves traveling through both the central and edge chains (sensor 2D in Fig. 5(b)) to determine if existing imperfections in the granular crystal allowed for deviations from the expected wave propagation paths. For the edge chains, the difference in time of arrival of peak particle acceleration ($t_{\text{peak}}(2B) - t_{\text{peak}}(2A)$) was $-0.50(\pm 6.5)$ microseconds and the percent difference in peak acceleration of sensor $2A$ with respect to sensor $2B$ was $-7\%(\pm 18\%)$. The experimental results shown in Fig. 5(b) best represent the average response of the system from the 15 repeated experiments in terms of the relative arrival times and amplitudes at sensor locations 2A and 2B. We observed, as expected, that the sensor away from the traveling waves (sensor 2D) was not measurably excited by the impact (Fig. 5).

Experiments and numerical simulations were performed also for crystals excited by out-of-plane impacts. Results from this analysis are reported in Figs. 6 and 7. In this configuration, we observed identical solitary waves traveling through the 8 central chains of the granular crystal, forming cross-shaped propagation beams (Fig. 6). Numerical simulations revealed that of the total energy input into the system (by the striker spheres initial velocity), 44.3% went into the solitary waves traveling in the eight central chains, 8.0% was lost in the rebounding of the striker particles, 47.7% was lost in the rebound of the four

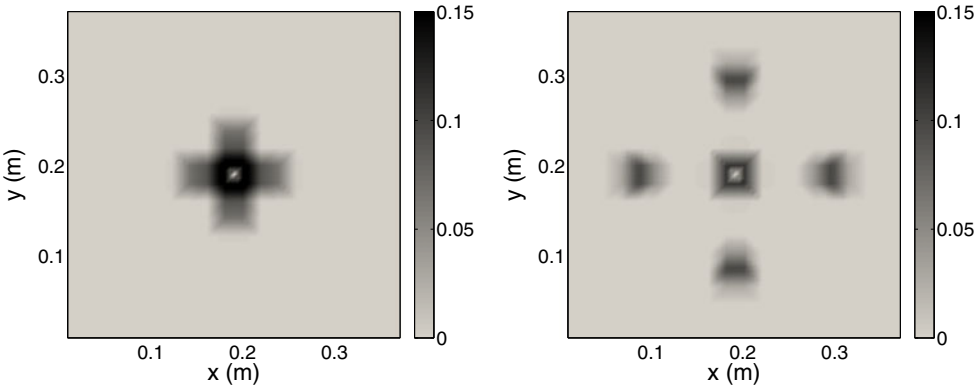

Fig. 6 Density plots corresponding to the amplitude of the particle velocity obtained from numerical simulations as a function of spacial position in the granular crystal. (*Left*) At 0.15 ms and (*Right*) at 0.30 ms after the array was impacted out-of-plane with a striker velocity $V_z = -0.65$ m/s. The *grey-scale* indicates the particle velocity amplitude in m/s

initially impacted central spheres. Sensors 3A and 3B were placed six particles from the out-of-plane impact in two of the central chains and sensor 3C was located eight particles from the impact in one of the central chains (Fig. 7(a)). To determine if existing experimental imperfections in the granular crystal allowed for deviations from the expected wave propagation paths, we positioned an additional sensor (sensor 3D in Fig. 7(a)) five particles away from the central chains of the crystal. The particle acceleration measured by the sensors and their motion was compared with numerical simulations (Fig. 7). Experiments were repeated 15 times, with an average striker velocity of $V_z = -0.65$ m/s.

Slight variations in solitary wave amplitudes and arrival times were again observed between adjacent spheres in experiments. The difference in time of arrival of peak particle acceleration ($t_{\text{peak}}\,(3B) - t_{\text{peak}}\,(3A)$) was on average 25($\pm$54) microseconds and the percent difference in peak acceleration of sensor 3A with respect to sensor 3B was 1%($\pm$42%). The experiments plotted in Fig. 7 most closely represent the average response of the system. As with the in-plane impact, we observed that the sensor away from the traveling waves was not measurably affected by the waves traveling in the central chains. The lack of particle motion at sensors 2D (Fig. 5) and 3D (Fig. 7) and the good agreement with simulation and experimental results indicate that any existing deviations from the granular crystal's ideal contact lattice were not significant enough to leak energy from excited chains or to prevent the observed solitary waves from forming.

The presence of dissipation is evident in the experimental results. This leads to an observable discrepancy in the wave amplitude between the signal recorded in experiments and in numerical simulations (that do not include dissipative losses). In highly nonlinear systems, the wave propagation speed is a function of the wave amplitude. As a consequence, the noticeable travel

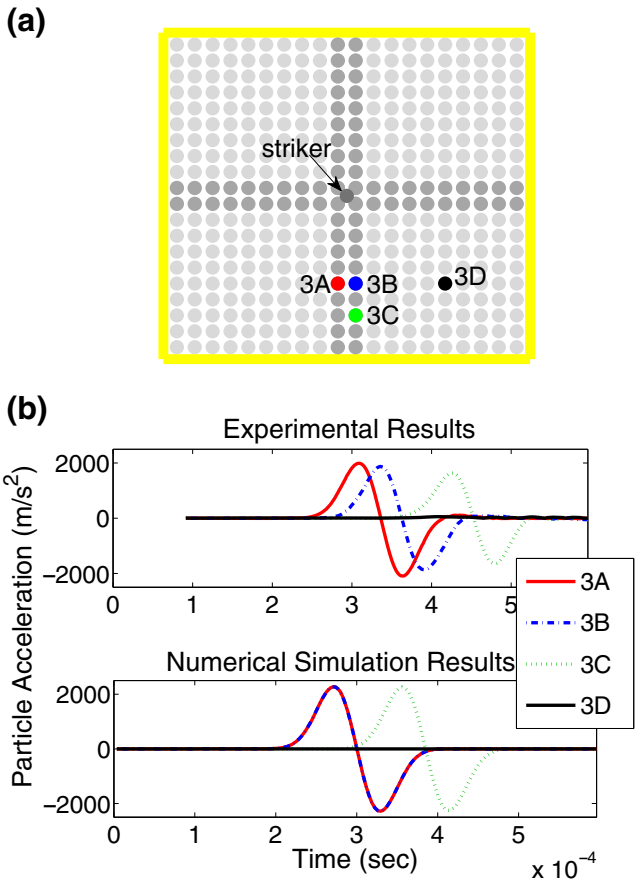

Fig. 7 Experimental and numerical simulation responses of the central chains in the granular crystal resulting from an out-of-plane impact. (**a**) Schematic diagram showing the experimental setup and the positions of the sensor particles (*shaded spheres* indicate particles excited by the impulse). (**b**) Signals recorded at the sensor locations. The *top panel* represents experimental results and the *bottom panel* the numerical simulations. In both simulations and experiments the particle's acceleration in the negative y-direction is plotted as a function of time. The experimental x-acceleration was nearly zero for all sensor locations (zero in simulations) and was therefore not plotted. The signal plotted for sensor 3D includes the total magnitude of the x- and y-particle acceleration

time difference observed between the pulses recorded experimentally and the ones obtained from numerical simulations can be also attributed to the signal attenuation due to dissipation. We observed significantly more dissipation in the waves traveling through the edge chains (Fig. 5) compared with those traveling through central chains in the granular crystal (Figs. 4 and 7). This difference could be attributed to the fact that edge particles are in contact with two walls (side and bottom), compared to only one wall (bottom) for internal particles, introducing more friction and increasing the rate of amplitude decay.

Particle Velocity - Wave Speed Scaling Relation

A scaling relation between the particle velocity and the propagating wave speed was determined by separately inspecting the waves traveling through each of the chains involved in the signal propagation. The results were compared with the scaling relationship available from the one-dimensional highly nonlinear wave theory [1, 2]. To determine the experimental particle velocity, we numerically integrated the measured particle acceleration. The peak value of the particle velocity was then plotted against the calculated wave speed for a variety of striker velocities (see the points in Figs. 8, 9, and 10). We compared the experimental values with data computed with our discrete element model, performing simulations for different striker velocities.

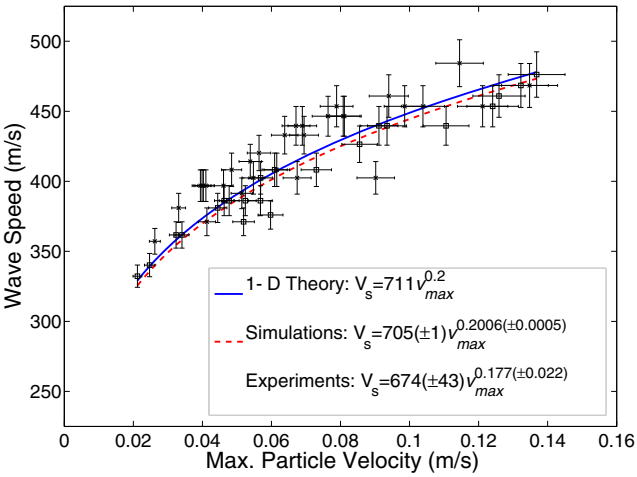

Fig. 9 Wave speed vs. maximum particle velocity for the edge chains when the system is impacted in-plane. The *squares* denote tests for sensor locations 2B and 2C, while the *stars* denote tests when sensors are moved to the opposite chain (2A and the respective neighboring particle of 2C, location X_1Y_{18}). Results of the linear regression on the log-log data for both experiments and simulations are shown (with 95% confidence intervals)

The experimental peak particle velocities (Figs. 8–10) were calculated by averaging the peak values from the sensor pairs. The plotted experimental wave speed was calculated from the time of flight between the two sensors' peak velocities (t) and the distance between the sensor particles' centers (d). Error bars in the wave speed direction were calculated based on bead tolerances (±0.01 mm, Δd) and the sampling

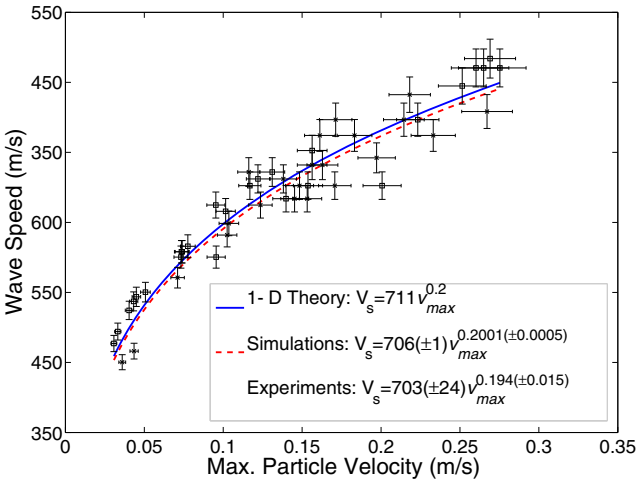

Fig. 8 Wave speed vs. maximum particle velocity for the central chains when the system is impacted in-plane. The *squares* denote tests for sensor locations 1B and 1C, while the *stars* denote tests when sensors are moved to the adjacent chain (1A and the respective neighboring particle of 1C, location $X_{15}Y_{10}$). Results of the linear regression on the log-log data for both experiments and simulations are shown (with 95% confidence intervals)

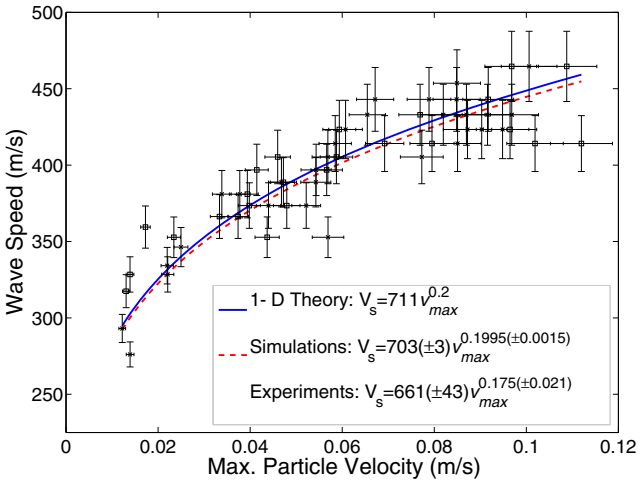

Fig. 10 Wave speed vs. maximum particle velocity for the central chains when the system is impacted out-of-plane. The *squares* denote tests for sensor locations 3B and 3C, while the *stars* denote tests when sensors are moved to the adjacent chain (3A and the respective neighboring particle of 3C, location $X_{10}Y_3$). Results of the linear regression on the log-log data for both experiments and simulations are shown (with 95% confidence intervals)

rate (2 microseconds between data points, Δt). Since wave speed, V_s, is d/t, we can write $\frac{dV_s}{V_s} = \frac{\frac{\partial V_s}{\partial t}dt + \frac{\partial V_s}{\partial d}dd}{d/t}$ or letting $dx \rightarrow \triangle x$, we get error bars extending in each direction with length $\triangle V_s = (\frac{\triangle t}{t} + \frac{\triangle d}{d}) \cdot V_s$. In the maximum particle velocity direction, error bars were calculated based on uncertainty in the sensors' calibration factors (3%, ΔK) and sensor misalignment (it was conservatively assumed that sensors could be aligned, by hand, within 10 degrees of the true x-, y-, and z-directions, ΔV). Similarly, since acceleration, a, is V/K, we can again get the integrated velocity error bar length in each direction from $\triangle a = (\frac{\triangle V}{V} + \frac{\triangle K}{K}) \cdot a$. Here V represents the measured voltage from accelerometers and K the calibration factor. The error bars did not take into account phenomenon such as the presence of gaps in the granular crystal, which could explain data points residing far from the theoretical and simulation lines.

A linear regression was performed for both numerical simulations and experimental data points (on a log-log scale) to determine the amplitude-wave speed relationship for traveling waves due to both the in-plane and out-of-plane impacts (Figs. 8–10). We observed that the wave behavior in this simple two-dimensional system generally follows the same $V_s \, \alpha \, v_{\max}^{1/5}$ relationship that was derived for one-dimensional systems [2].

Pulse Length

The wavelength of the observed solitary waves was calculated by separately inspecting the waves traveling through each of the chains described above. In experiments, we calculated the solitary wave length following two approaches. The values obtained were then compared with one-dimensional theoretical values. In the first approach we fit the experimental signals to the theoretical waveforms [1, 2]. In the second approach, we directly calculated the wavelength at half maximum amplitude (full width at half maximum values).

From Nesterenko's one-dimensional theory the particle velocity profile in a highly nonlinear chain of spheres approximately follows equation (2), thus the acceleration profile follows $a = V_s(\frac{5V_s^2}{2c^2})^2 \frac{\sqrt{10}}{10R} \cos^3(\frac{\sqrt{10}}{10R}x) \sin(\frac{\sqrt{10}}{10R}x)$. The normalized experimental acceleration data was fit (in a nonlinear least squares sense) to the waveform, $a = \cos^3(\frac{2\pi(t-t_o)}{\lambda}) \sin(\frac{2\pi(t-t_o)}{\lambda})$, with fitting parameters t_o and λ, and the solitary wavelength was then calculated as λ/2. For comparison, the integrated velocity profiles were also fit to the more familiar $v = \cos^4(\frac{2\pi(t-t_o)}{\lambda})$ waveform, and the wavelength was again calculated as λ/2. The calculated wavelengths were multiplied by the measured wave speed to obtain the wavelength in units of length. The comparison with one-dimensional theory, numerical simulations, and experiments of the fitted wavelength can be seen in Fig. 11(a) and (b). The comparison of wavelength at half maximum amplitude for one-dimensional theory, numerical simulations, and experiments can be seen in Fig. 11(c) and (d), where the full width at half maximum values of the acceleration and velocity waveforms are plotted as a function of distance from impact, respectively.

In general, the experimental wavelengths are in reasonable agreement with the numerical simulations. There is a clear discrepancy between the theoretical wavelength (based on the wave shape given by equation (1)), and the stabilized waveform from numerical simulations. However, a similar decrease (approximately 13%) in the full width at half maximum values can also be seen when comparing Chatterjee's [7] asymptotic solution for the shape of the solitary wave with Nesterenko's theory (equation (2)). In simulations, it appears that the wave reaches a stable waveform after

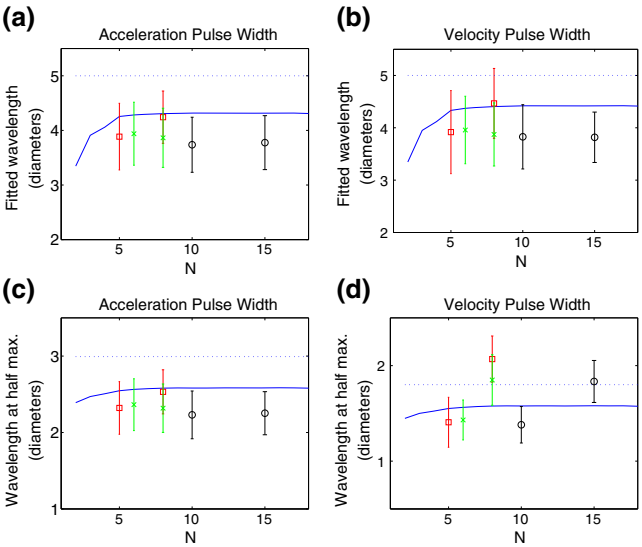

Fig. 11 Wavelength of the solitary wave as a function of distance from the impact (N). The *dotted lines* represent the theoretical values from Nesterenko's long wavelength approximation and the *solid lines* represent a smoothed curve through simulation data. *Circles* represent data from sensor locations 1C and 1D (Fig. 4) and *squares* represent data from sensor locations 2B and 2C (Fig. 5) after the array was impacted in-plane. The *crosses* represent data from sensor locations 3B and 3C (Fig. 7) after the array was impacted out-of-plane. (**a**) Wavelength calculated by fitting the acceleration curves to Nesterenko's waveform. (**b**) Wavelength calculated by fitting the (integrated) velocity curves to Nesterenko's waveform (equation (2)). (**c**) Wavelength at half maximum amplitude directly calculated from the acceleration profiles. (**d**) Wavelength at half maximum amplitude directly calculated from the (integrated) velocity data. *Error bars* extend two standard deviations from the mean values

traveling through roughly five or six particles from the impact location. In experiments, the pulse temporal length is observed to increase with increasing distance from the point of impact. This effect can be related to the presence of dissipation.

Conclusions

We developed a new experimental measurement technique for measuring the multi-directional acceleration of particles in a granular crystal. We demonstrated good agreement between experimental results and numerical simulation results based on a Hertzian discrete particle model. We observed that when the two-dimensional square packing of steel spheres was impacted in-plane (between two edge particles) or out-of-plane (simultaneously impacting four central particles), the impulsive excitation was resolved into solitary waves traveling only down initially excited chains. We observed that deviations from the granular crystal's ideal contact lattice were not significant enough to prevent the formation and propagation of solitary waves, with no or minor energy lost in the excitation of adjacent chains of particles. The observed solitary waves appeared to have comparable (Hertzian) properties to the extensively studied solitary waves traveling in an uncompressed, one-dimensional chain of spheres. These finding can be used in the design of new materials with controllable dynamic properties.

Acknowledgements We thank Dr. A. Spadoni for his suggestions in the design of the confining box used in experiments. We also thank R. Giordano and A. Esposito for their preliminary work on the subject. This work was supported by an award from the Department of Energy Office of Science (DOE SCGF) and the Army Research Office MURI (Dr. David Stepp).

References

1. Nesterenko V (1983) Propagation of nonlinear compression pulses in granular media. J Appl Mech Tech Phys 24:733
2. Nesterenko VF (2001) Dynamics of heterogeneous materials. Springer, New York
3. Lazaridi A, Nesterenko V (1985) Observation of a new type of solitary waves in a one-dimensional granular medium. J Appl Mech Tech Phys 26:405
4. Coste C, Falcon E, Fauve S (1997) Solitary waves in a chain of beads under Hertz contact. Phys Rev E 56:6104
5. Coste C, Gilles B (1999) On the validity of Hertz contact law for granular material acoustics. Eur Phys J B 7:155
6. Daraio C, Nesterenko VF, Herbold EB, Jin S (2005) Strongly nonlinear waves in a chain of Teflon beads. Phys Rev E 72:016603
7. Chatterjee A (1999) Asymptotic solution for solitary waves in a chain of elastic spheres. Phys Rev E 59:5912
8. Nakagawa M, Agui J, Wu D, Extramiana D (2003) Impulse dispersion in a tapered granular chain. Granul Matter 4: 167
9. Sen S, Manciu F, Manciu M (2001) Thermalizing an impulse. Physica A 299:551
10. Nesterenko V, Lazaridi A, Sibiryakov E (1995) The decay of soliton at the contact of two "acoustic vacuums". J Appl Mech Tech Phys 36:166
11. Vergara L (2005) Scattering of solitary waves from interfaces in granular media. Phys Rev Lett 95:108002
12. Nesterenko V, Daraio C, Herbold E, Jin S (2005) Anomalous wave reflection at the interface of two strongly nonlinear granular media. Phys Rev Lett 95:158702
13. Job S, Melo F, Sokolow A, Sen S (2007) Solitary wave trains in granular chains: experiments, theory and simulations. Granul Matter 10:13
14. Hascoët E, Herrmann H, Loreto V (1999) Shock propagation in a granular chain. Phys Rev E 59:3202
15. Job S, Santibanez F, Tapia F, Melo F (2009) Wave localization in strongly nonlinear Hertzian chains with mass defect. Phys Rev E 80:25602
16. Job S, Melo F, Sokolow A, Sen S (2005) How Hertzian solitary waves interact with boundaries in a 1D granular medium. Phys Rev Lett 94:178002
17. Daraio C, Nesterenko V, Herbold E, Jin S (2006) Energy trapping and shock disintegration in a composite granular medium. Phys Rev Lett 96:058002
18. Hinch E, Saint-Jean S (1999) The fragmentation of a line of balls by an impact. Proc R Soc Lond A 455:3201
19. Manciu M, Sen S, Hurd A (2000) Crossing of identical solitary waves in a chain of elastic beads. Phys Rev E 63: 016614
20. Daraio C, Nesterenko V, Herbold E, Jin S (2006) Tunability of solitary wave properties in one-dimensional strongly nonlinear phononic crystals. Phys Rev E 73:026610
21. Sinkovits R, Sen S (2003) Nonlinear dynamics in granular columns. Phys Rev Lett 74:2686
22. Gilles B, Coste C (2003) Low-frequency behavior of beads constrained on a lattice. Phys Rev Lett 90:174302
23. Velický B, Caroli C (2002) Pressure dependence of the sound velocity in a two-dimensional lattice of Hertz–Mindlin balls: mean-field description. Phys Rev E 65(2):021307
24. Goddard J (1990) Nonlinear elasticity and pressure-dependent wave speeds in granular media. Proc R Soc Lond, A Math Phys Sci 430:105
25. Zhu Y, Shukla A, Sadd M (1996) The effect of microstructural fabric on dynamic load transfer in two dimensional assemblies of elliptical particles. J Mech Phys Solids 44: 1283
26. Sadd M, Gao J, Shukla A (1997) Numerical analysis of wave propagation through assemblies of elliptical particles. Comput Geotech 20:323
27. Nishida M, Tanaka K, Ishida T (2009) DEM simulation of wave propagation in two-dimensional ordered array of particles. Shock Waves 815:357
28. Nishida M, Tanaka Y (2010) DEM simulations and experiments for projectile impacting two-dimensional particle packings including dissimilar material layers. Granul Matter 12:357
29. Merkel A, Tournat V, Gusev V (2010) Elastic waves in noncohesive frictionless granular crystals. Ultrasonics 50:133
30. Sen S, Sinkovits R (1996) Sound propagation in impure granular columns. Phys Rev E 54:6857
31. Sadd M, Tai Q, Shukla A (1993) Contact law effects on wave propagation in particulate materials using distinct element modeling. Int J Non-Linear Mech 28:251

32. Daraio C, Ngo D, Nesterenko V, Fraternali F (2010) H ighly nonlinear pulse splitting and recombination in a two-dimensional granular network. Phys Rev E 82:036603
33. Shukla A, Zhu C, Sadd M (1988) Angular dependence of dynamic load transfer due to explosive loading in granular aggregate chains. J Strain Anal Eng Des 23:121
34. Shukla A, Sadd M, Singh R, Tai Q, Vishwanathan S (1993) Role of particle shape and contact profile on the dynamic response of particulate materials. Opt Lasers Eng 19:99
35. Bardenhagen S, Brackbill J (1998) Dynamic stress bridging in granular material. J Appl Phys 83:5732
36. Geng J, Reydellet G, Clément E, Behringer R (2003) Green's function measurements of force transmission in 2D granular materials. Physica D: Nonlinear Phenom 182: 274
37. Johnson K (1987) Contact mechanics. The Press Syndicate of the University of Cambridge, The Pitt Building
38. Hong J, Xu A (2001) Effects of gravity and nonlinearity on the waves in the granular chain. Phys Rev E 63:061310
39. Carretero-González R, Khatri D, Porter M, Kevrekidis P, Daraio C (2009) Dissipative solitary waves in granular crystals. Phys Rev Lett 102:024102